

Parametric resonance characteristics of angle-ply twisted curved panels

— [Source link](#) 

Shishir Kumar Sahu, A. V. Asha

Institutions: National Institute of Technology, Rourkela

Published on: 01 Mar 2008 - International Journal of Structural Stability and Dynamics (World Scientific Publishing Company)

Topics: Rotary inertia and Instability

Related papers:

- [Parametric Instability of Composite Curved Panel Subjected to Concentrated Edge Loading](#)
- [Dynamic stability of curved panels with cutouts](#)
- [Parametric instability of thick doubly curved CNT reinforced composite sandwich panels under in-plane periodic loads using higher-order shear deformation theory:](#)
- [Parametric instability of doubly curved panels subjected to non-uniform harmonic loading](#)
- [Parametric instability of laminated composite shear-deformable flat panels subjected to in-plane edge loads](#)

Share this paper:    

View more about this paper here: <https://typeset.io/papers/parametric-resonance-characteristics-of-angle-ply-twisted-c1dy5zhe6y>

International Journal of Structural Stability and Dynamics
(IJSSD) (2008)

<http://dx.doi.org/10.1142/S0219455408002557>

**PARAMETRIC RESONANCE CHARACTERISTICS OF ANGLE-PLY TWISTED
CURVED PANELS**

Author's post-print

Archived in dspace@nitrr.edu

Parametric Resonance Characteristics of Angle-ply Twisted Curved Panels

S. K. Sahu* and A.V. Asha

*Department of Civil Engineering, National Institute of Technology,
Rourkela, Orissa-769008 (INDIA). Email: rssksahu@yahoo.com*

Abstract: The present study deals with the dynamic stability of laminated composite pre-twisted cantilever panels. The effects of various parameters on the principal instability regions are studied using Bolotin's approach and finite element method. The first order shear deformation theory is used to model the twisted curved panels, considering the effects of transverse shear deformation and rotary inertia. The results on the dynamic stability studies of the laminated composite pre-twisted panels suggest that the onset of instability occurs earlier and the width of dynamic instability regions increase with introduction of twist in the panel. The instability occurs later for square than rectangular twisted panels. The onset of instability occurs later for pre-twisted cylindrical panels than the flat panels due to addition of curvature. However, the spherical pre-twisted panels show small increase of non-dimensional excitation frequency.

Keywords: Twisted panels, dynamic stability, composites, instability regions

1. INTRODUCTION

The twisted cantilever panels have significant applications in wide chord turbine blades, compressor blades, fan blades, particularly in gas turbines. This range of practical applications demands a proper understanding of their vibration, static and dynamic stability characteristics. Due to its significance, a large number of references deal with the free vibration of twisted plates. The blades are subjected to axial periodic forces due to axial components of aerodynamic or hydrodynamic forces acting on the blades. Structural elements subjected to in-plane periodic

* Corresponding author. E-mail address: rssksahu@yahoo.com, sksahu@nitrrkl.ac.in

forces may lead to parametric resonance, due to certain combinations of the values of load parameters. The instability may occur below the critical load of the structure under compressive loads over wide ranges of excitation frequencies. Composite materials are being increasingly used in turbo-machinery blades because of their specific strength, stiffness and these can be tailored through the variation of fiber orientation and stacking sequence to obtain an efficient design. Thus the parametric resonance characteristics of laminated composite twisted cantilever panels are of great importance for understanding the systems under periodic loads.

An excellent survey of the earlier works in the free vibration of turbo-machinery blades was carried out by Leissa [1] through 1981. The vast majority of earlier researches treated the blades as beams i.e. one-dimensional case. Such an idealization is highly inaccurate for the blade with moderate to low aspect ratio. Leissa, Lee and Wang [2] employed shallow shell theory and Ritz method to determine the frequencies of vibration of turbo-machinery blades with twist for different degrees of shallowness and thickness. However, there are very few studies on free vibration of composite pre-twisted plates. Qatu and Leissa [3] investigated the free vibration of laminated composite twisted cantilever plates using Ritz method. Although extensive free vibration frequencies and mode shapes are studied, the results were however confined to symmetric laminates only. He, Lim and Kitipornchai [4] presented the free vibration of symmetric as well as anti-symmetric laminates explaining the limit of linear twisting curvature. Karmakar and Sinha [5] analyzed the free vibration of laminated composite pre-twisted cantilever plates using finite element method. Hu *et al.*[6] studied the vibration of angle-ply laminated plates with twist using a Raleigh-Ritz procedure. Kee and Kim [7] analysed the vibration characteristics of initially twisted rotating shell type composite blades. Lee *et al.*[8] studied the vibration of twisted cantilevered conical composite shells, using finite element method based on the Hellinger-Reissner principle. Hu *et al.* [9] have also investigated the

vibration of twisted laminated composite conical shells by the energy method. Since Bolotin [10] introduced the subject of dynamic stability under periodic loads, the topic has attracted much interest. This monograph explained the general theory of dynamic stability of elastic systems of deriving the coupled second order differential equation of the Mathieu-Hill type and the determination of the regions of instability by seeking periodic solution using Fourier series expansion. The parametric instability characteristics of laminated composite non-twisted plates were studied by a number of investigators [11-14]. Ganapathi *et al.* [15] investigated the dynamic stability of composite curved panels without twist subjected to uniform in-plane periodic loads. Sahu and Datta [16] studied the parametric excitation behaviour of doubly curved untwisted panels subjected to non-uniform in-plane harmonic loading. A few studies were made to investigate the dynamic stability of twisted blades. Ray and Kar [17] analyzed the dynamic stability of pre-twisted sandwich beams. Chen and Peng [18] studied the dynamic stability of twisted rotating blades, using the Galerkin finite element method. Lin and Chen [19] studied the stability problems of a pre-twisted blade with a constrained viscoelastic core subjected to a periodic axial load, using a 2-node element neglecting shear deformation and rotary inertia. The above studies involved dynamic stability of twisted structures using beam idealization. The study on stability characteristics of twisted panels is new. Crispino and Benson [20] investigated on the stability of thin, rectangular, orthotropic plates which were in a state of tension and twist using transfer matrix method. Recently, Sahu *et al.* [21] analyzed the buckling behaviour of twisted cantilever panels using finite element method. In the present investigation, the parametric instability characteristics of laminated composite pre-twisted cantilever flat and curved panels subjected to in-plane harmonic loads are studied. The effects of angles of pre-twist, aspect ratio, static load factor, and the lamination parameters of the composite twisted curved panels on the principal instability regions are studied in this investigation.

2. MATHEMATICAL FORMULATIONS

The basic configuration of the problem studied here is a cantilever panel of length 'a' and 'b', twisted through an angle ϕ , as shown in Fig.1 and subjected to in-plane periodic edge loading.

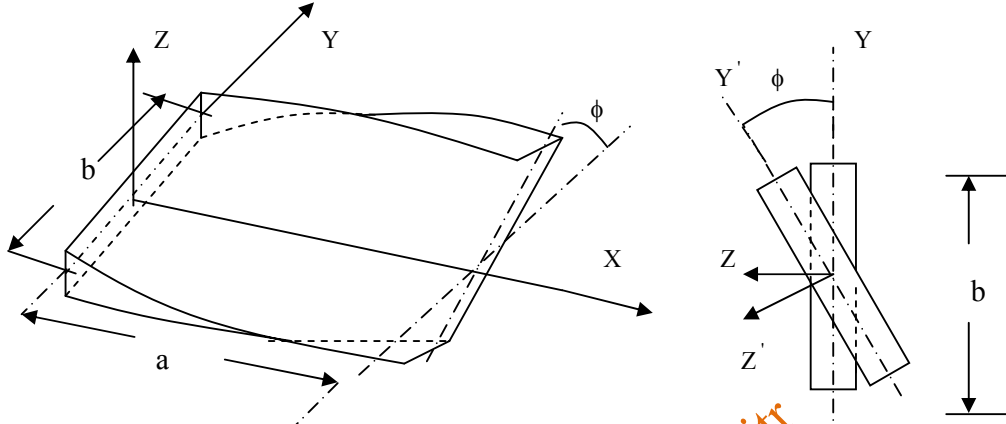


Fig. 1 Geometry and co-ordinate systems of twisted cantilever plates.

Governing Equations: The governing differential equations for vibration of a shear deformable laminated composite twisted cantilever panel subjected to in-plane loads are [22, 23]:

$$\begin{aligned}
 \frac{\partial N_x}{\partial x} + \frac{\partial N_{xy}}{\partial y} - \frac{1}{2} \left(\frac{1}{R_y} - \frac{1}{R_x} \right) \frac{\partial M_{xy}}{\partial y} + \frac{Q_x}{R_x} + \frac{Q_y}{R_{xy}} &= P_1 \frac{\partial^2 u}{\partial t^2} + P_2 \frac{\partial^2 \theta_x}{\partial t^2} \\
 \frac{\partial N_{xy}}{\partial x} + \frac{\partial N_y}{\partial y} + \frac{1}{2} \left(\frac{1}{R_y} - \frac{1}{R_x} \right) \frac{\partial M_{xy}}{\partial x} + \frac{Q_y}{R_y} + \frac{Q_x}{R_{xy}} &= P_1 \frac{\partial^2 v}{\partial t^2} + P_2 \frac{\partial^2 \theta_y}{\partial t^2} \\
 \frac{\partial Q_x}{\partial x} + \frac{\partial Q_y}{\partial y} - \frac{N_x}{R_x} - \frac{N_y}{R_y} - 2 \frac{N_{xy}}{R_{xy}} + N_x^0 \frac{\partial^2 w}{\partial x^2} + N_y^0 \frac{\partial^2 w}{\partial y^2} &= P_1 \frac{\partial^2 w}{\partial t^2} \\
 \frac{\partial M_x}{\partial x} + \frac{\partial M_{xy}}{\partial y} - Q_x &= P_3 \frac{\partial^2 \theta_x}{\partial t^2} + P_2 \frac{\partial^2 u}{\partial t^2} \\
 \frac{\partial M_{xy}}{\partial x} + \frac{\partial M_y}{\partial y} - Q_y &= P_3 \frac{\partial^2 \theta_y}{\partial t^2} + P_2 \frac{\partial^2 v}{\partial t^2}
 \end{aligned} \tag{1}$$

Where N_x , N_y and N_{xy} are the in-plane stress resultants, M_x , M_y and M_{xy} are moment resultants and Q_x , Q_y = transverse shear stress resultants. R_x , R_y and R_{xy} identify the radii of curvatures in the x and y direction and *radius of twist*.

$$(P_1, P_2, P_3) = \sum_{k=1}^n \int_{z_{k-1}}^{z_k} (\rho)_k (1, z, z^2) dz \quad (2)$$

Where n= number of layers of laminated composite twisted curved panel, $(\rho)_k$ =mass density of k_{th} layer from mid-plane.

Dynamic stability studies: The equation of motion for vibration of a laminated composite twisted cantilever panel, subjected to in-plane loads can be expressed in the matrix form as:

$$[M]\{\ddot{q}\} + [[K_e] - N(t)[K_g]]\{q\} = 0 \quad (3)$$

‘q’ is the vector of degrees of freedoms (u, v, w, θ_x , θ_y). The in-plane load ‘N(t)’ may be harmonic and can be expressed in the form:

$$N(t) = N_s + N_t \cos \Omega t \quad (4)$$

Where N_s is the static portion of load N(t), N_t the amplitude of the dynamic portion of N(t) and Ω is the frequency of the excitation. The stress distribution in the panel may be periodic.

Considering the static and dynamic component of load as a function of the critical load,

$$N_s = \alpha N_{cr}, \quad N_t = \beta N_{cr} \quad (5)$$

Where α and β are the static and dynamic load factors respectively. Using Eq.(5), the equation of motion for twisted curved panel under periodic loads in matrix form may be obtained as:

$$[M]\{\ddot{q}\} + [[K_e] - \alpha N_{cr}[K_g] - \beta N_{cr}[K_g] \cos \Omega t]\{q\} = 0 \quad (6)$$

The above Eq. (6) represents a system of differential equations with periodic coefficients of the Mathieu-Hill type. The development of regions of instability arises from Floquet’s theory which establishes the existence of periodic solutions of periods T and 2T. The boundaries of the

primary instability regions with period $2T$, where $T=2\pi/\Omega$ are of practical importance [10] and the solution can be achieved in the form of the trigonometric series:

$$q(t) = \sum_{k=1,3,5,\dots}^{\infty} [\{a_k\} \sin(k\Omega t / 2) + \{b_k\} \cos(k\Omega t / 2)] \quad (7)$$

Putting this in Eq.(6) and if only first term of the series is considered, equating coefficients of $\sin \Omega t/2$ and $\cos \Omega t/2$, the equation (6) reduces to

$$[[K_e] - \alpha P_{cr}[K_g] \pm \frac{1}{2} \beta P_{cr}[K_g] - \frac{\Omega^2}{4}[M]] \{q\} = 0 \quad (8)$$

Eq.(8) represents an eigenvalue problem for known values of α , β and P_{cr} . The two conditions under the plus and minus sign correspond to two boundaries of the dynamic instability region. The eigenvalues are Ω , which give the boundary frequencies of the instability regions for given values of α and β . In this analysis, the computed static buckling load of the panel is considered as the reference load.

Finite Element Formulation: A Finite element analysis was performed using an eight noded curved isoparametric shell element with five degrees of freedom u , v , w , θ_x and θ_y per node. The shell element is modified to accommodate laminated materials and twisting of the panel, based on first order shear deformation theory. u , v and w are the displacement components in the x , y , z directions and θ_x and θ_y are the rotations.

Strain Displacement Relations: Green-Lagrange's strain displacement relations are presented in general throughout the analysis. The linear part of the strain is used to derive the elastic stiffness matrix and the non-linear part of the strain is used to derive the geometric stiffness matrix. The total strain is given by

$$\{\varepsilon\} = \{\varepsilon_l\} + \{\varepsilon_{nl}\} \quad (9)$$

The linear shear deformable Sanders' strain displacement relations are [22]:

$$\begin{aligned}
\varepsilon_{xl} &= \frac{\partial u}{\partial x} + \frac{w}{R_x} + zk_x \\
\varepsilon_{yl} &= \frac{\partial v}{\partial y} + \frac{w}{R_y} + zk_y \\
\gamma_{xyl} &= \frac{\partial u}{\partial y} + \frac{\partial v}{\partial x} + \frac{2w}{R_{xy}} + zk_{xy} \\
\gamma_{xzl} &= \frac{\partial w}{\partial x} + \theta_x - \frac{u}{R_x} - \frac{v}{R_{xy}} \\
\gamma_{yzl} &= \frac{\partial w}{\partial y} + \theta_y - \frac{v}{R_y} - \frac{u}{R_{xy}}
\end{aligned} \tag{10}$$

The bending strains k_j are expressed as,

$$\begin{aligned}
k_x &= \frac{\partial \theta_x}{\partial x}, \quad k_y = \frac{\partial \theta_y}{\partial y} \\
k_{xy} &= \frac{\partial \theta_x}{\partial y} + \frac{\partial \theta_y}{\partial x} + \frac{1}{2} \left(\frac{1}{R_x} - \frac{1}{R_y} \right) \left(\frac{\partial v}{\partial x} - \frac{\partial u}{\partial y} \right)
\end{aligned} \tag{11}$$

The non-linear strain components are as follows:

$$\begin{aligned}
\varepsilon_{xnl} &= \frac{1}{2} \left(\frac{\partial u}{\partial x} \right)^2 + \frac{1}{2} \left(\frac{\partial v}{\partial x} \right)^2 + \frac{1}{2} \left(\frac{\partial w}{\partial x} - \frac{u}{R_x} \right)^2 + \frac{1}{2} z^2 \left[\left(\frac{\partial \theta_x}{\partial x} \right)^2 + \left(\frac{\partial \theta_y}{\partial x} \right)^2 \right] \\
\varepsilon_{ynl} &= \frac{1}{2} \left(\frac{\partial u}{\partial y} \right)^2 + \frac{1}{2} \left(\frac{\partial v}{\partial y} \right)^2 + \frac{1}{2} \left(\frac{\partial w}{\partial y} - \frac{v}{R_y} \right)^2 + \frac{1}{2} z^2 \left[\left(\frac{\partial \theta_x}{\partial y} \right)^2 + \left(\frac{\partial \theta_y}{\partial y} \right)^2 \right] \\
\gamma_{xynl} &= \frac{\partial u}{\partial x} \left(\frac{\partial u}{\partial y} \right) + \frac{\partial v}{\partial x} \left(\frac{\partial v}{\partial y} \right) + \left(\frac{\partial w}{\partial x} - \frac{u}{R_x} \right) \left(\frac{\partial w}{\partial y} - \frac{v}{R_y} \right) + z^2 \left[\left(\frac{\partial \theta_x}{\partial x} \right) \left(\frac{\partial \theta_x}{\partial y} \right) + \left(\frac{\partial \theta_y}{\partial x} \right) \left(\frac{\partial \theta_y}{\partial y} \right) \right]
\end{aligned} \tag{12}$$

Constitutive Relations: The laminated composite pre-twisted cantilever panel is considered to be composed of composite material laminae (typically thin layers). The material of each lamina consists of parallel continuous fibers embedded in a matrix. Each layer is regarded as on a

microscopic scale as being homogenous and orthotropic. The stress resultants are related to the mid-plane strains and curvatures for the laminated shell element as :

$$\{\sigma\} = [D]\{\varepsilon\}$$

or

$$\begin{Bmatrix} N_i \\ M_i \\ Q_i \end{Bmatrix} = \begin{bmatrix} A_{ij} & \dots & B_{ij} & \dots & 0 \\ B_{ij} & \dots & D_{ij} & \dots & 0 \\ 0 & \dots & 0 & \dots & S_{ij} \end{bmatrix} \begin{Bmatrix} \varepsilon_j \\ k_j \\ \gamma_m \end{Bmatrix} \quad (13)$$

The extensional, bending-stretching coupling and bending stiffnesses are expressed as

$$(A_{ij}, B_{ij}, D_{ij}) = \sum_{k=1}^n \int_{Z_{k-1}}^{Z_k} (\overline{Q}_{ij})_k (1, z, z^2) dz \quad i, j = 1, 2, 6 \quad (14)$$

The transverse shear stiffness is expressed as:

$$(S_{ij}) = \sum_{k=1}^n \int_{Z_{k-1}}^{Z_k} \kappa (\overline{Q}_{ij})_k dz \quad i, j = 4, 5 \quad (15)$$

Where κ is the transverse shear correction factor

The off-axis stiffness values are:

$$\begin{aligned} \overline{Q}_{11} &= Q_{11}m^4 + 2(Q_{12} + 2Q_{66})m^2n^2 + Q_{22}n^4 \\ \overline{Q}_{12} &= (Q_{11} + Q_{22} - 4Q_{66})m^2n^2 + Q_{12}(m^4 + n^4) \\ \overline{Q}_{22} &= Q_{11}n^4 + 2(Q_{12} + 2Q_{66})m^2n^2 + Q_{22}m^4 \\ \overline{Q}_{16} &= (Q_{11} - Q_{12} - 2Q_{66})m^3n + (Q_{12} - Q_{22} + 2Q_{66})n^3m \\ \overline{Q}_{26} &= (Q_{11} - Q_{12} - 2Q_{66})mn^3 + (Q_{12} - Q_{22} + 2Q_{66})m^3n \\ \overline{Q}_{66} &= (Q_{11} + Q_{22} - 2Q_{12} - 2Q_{66})m^2n^2 + Q_{66}(m^4 + n^4) \end{aligned} \quad (16)$$

The stiffness corresponding to transverse deformations are:

$$\begin{aligned} \overline{Q}_{44} &= G_{13}m^2 + G_{23}n^2 \\ \overline{Q}_{45} &= (G_{13} - G_{23})mn \\ \overline{Q}_{55} &= G_{13}n^2 + G_{23}m^2 \end{aligned} \quad (17)$$

Where $m = \cos \theta$ and $n = \sin \theta$; and $\theta =$ angle between the arbitrary principal axis with the material axis in a layer. The on-axis stiffness are:

$$Q_{11} = \frac{E_{11}}{(1-\nu_{12}\nu_{21})}, Q_{12} = \frac{E_{11}\nu_{21}}{(1-\nu_{12}\nu_{21})}, Q_{21} = \frac{E_{22}\nu_{12}}{(1-\nu_{12}\nu_{21})}, Q_{22} = \frac{E_{22}}{(1-\nu_{12}\nu_{21})}, Q_{66} = G_{12} \quad (18)$$

Derivation of Element matrices: The element elastic stiffness and consistent mass matrices are derived using standard procedure as:

$$\begin{aligned} \text{Elastic stiffness matrix} \quad [k_e]_e &= \int_{-1}^1 \int_{-1}^1 [B]^T [D] [B] J |d\xi d\eta \\ \text{Consistent mass matrix} \quad [m]_e &= \int_{-1}^1 \int_{-1}^1 [N]^T [P] [N] J |d\xi d\eta \end{aligned} \quad (19)$$

Where [B], [D], are the strain-displacement matrix, stress-strain matrix and J is the Jacobian determinant. [N] is the shape function matrix and is expressed as:

$$[N] = \begin{bmatrix} N_i & 0 & 0 & 0 & 0 \\ 0 & N_i & 0 & 0 & 0 \\ 0 & 0 & N_i & 0 & 0 \\ 0 & 0 & 0 & N_i & 0 \\ 0 & 0 & 0 & 0 & N_i \end{bmatrix} \quad i=1,2,\dots,8$$

[P] involves mass density parameters as explained as:

$$[P] = \begin{bmatrix} P_1 & 0 & 0 & P_2 & 0 \\ 0 & P_1 & 0 & 0 & P_2 \\ 0 & 0 & P_1 & 0 & 0 \\ P_2 & 0 & 0 & P_3 & 0 \\ 0 & P_2 & 0 & 0 & P_3 \end{bmatrix}$$

Where P_1 , P_2 and P_3 are explained in Eq.(2). The geometric stiffness matrix is a function of in-plane stress distribution in the element due to applied edge loading. Plane stress analysis is carried out using the finite element techniques to determine the stresses and these are used to formulate the geometric stiffness matrix [22].

$$\text{Geometric stiffness matrix} \quad [k_g]_e = \int_{-1}^1 \int_{-1}^1 [G]^T [S] [G] J |d\xi d\eta \quad (20)$$

$$\text{Where } [S] = \begin{bmatrix} s & 0 & 0 & 0 & 0 \\ 0 & s & 0 & 0 & 0 \\ 0 & 0 & s & 0 & 0 \\ 0 & 0 & 0 & s & 0 \\ 0 & 0 & 0 & 0 & s \end{bmatrix} \quad \text{and} \quad [s] = \begin{bmatrix} \sigma_x^0 & \tau_{xy}^0 \\ \tau_{xy}^0 & \sigma_y^0 \end{bmatrix} = \frac{1}{h} \begin{bmatrix} N_x^0 & N_{xy}^0 \\ N_{xy}^0 & N_y^0 \end{bmatrix} \quad (21)$$

$$\left[\frac{\partial u}{\partial x}, \frac{\partial u}{\partial y}, \frac{\partial v}{\partial x}, \frac{\partial v}{\partial y}, \left(\frac{\partial w}{\partial x} - \frac{u}{R_x} \right), \left(\frac{\partial w}{\partial y} - \frac{v}{R_y} \right), \frac{\partial \theta_x}{\partial x}, \frac{\partial \theta_x}{\partial y}, \frac{\partial \theta_y}{\partial x}, \frac{\partial \theta_y}{\partial y} \right]^T = [G] \{u, v, w, \theta_x, \theta_y\} \quad (22)$$

A computer program is developed to perform all the necessary computations. Reduced integration technique is adopted to avoid possible shear locking. The overall matrices $[K_b]$, $[K_g]$ and $[M]$ are obtained by assembling the corresponding element matrices, using skyline technique. Subspace iteration method is adopted throughout to solve eigenvalue problems.

3. RESULTS AND DISCUSSIONS

Numerical results are presented for anti-symmetric angle-ply laminated pre-twisted cantilever panels with different combinations of lamination parameters and geometry including angle of twist, b/h ratio, aspect ratio and curvature. The clamped (C) boundary condition of the angle-ply panel using the first order shear deformation theory is:

C: $u=v=w=\theta_x=\theta_y=0$ at any edge.

Convergence study: The convergence studies are made for non-dimensional fundamental frequencies of vibration of square laminated composite twisted cantilever plates for two thickness ratios ($b/h=100, 20$) and three angles of twists ($\phi=0^0, 15^0$ and 30^0) for different mesh divisions and are shown in Table 1. The maximum difference between the second (8×8 mesh) and third (10×10 mesh) results is less than 0.1%, which indicates the sufficient convergence. From the above convergence study, 10×10 mesh has been employed to idealise the panel in the subsequent analysis.

Table 1 Convergence of non-dimensional fundamental frequencies of vibration of composite twisted cantilever plates with $[45^0 / -45^0 / 45^0]$ lamination.

$$\text{Non dimensional frequency, } \varpi = \omega a^2 \sqrt{(\rho / E_{11} h^2)}$$

$$a / b = 1, E_{11} = 138 \text{GPa}, E_{22} = 8.96 \text{GPa}, G_{12} = 7.1 \text{GPa}, \nu_{12} = 0.3$$

Mesh	Non-dimensional fundamental frequencies of free vibration for different thickness ratio and angles of twist					
	b/h=100			b/h=20		
	$\phi=0^0$	$\phi=15^0$	$\phi=30^0$	$\phi=0^0$	$\phi=15^0$	$\phi=30^0$
4×4	0.4615	0.5300	0.5165	0.4570	0.4744	0.4770
8×8	0.4596	0.5261	0.5123	0.4546	0.4719	0.4745
10×10	0.4592	0.5256	0.5118	0.4541	0.4714	0.4741

Comparison with previous studies: The accuracy and efficiency of the present finite element formulation is validated for free vibration analysis of composite twisted plates for different ply orientations with the results of Qatu & Leissa [3] and He, Lim and Kitipornchai [4] using Ritz method. The results are presented in Table 2, showing good comparison with the literature. To validate the formulation further, the principal instability regions of untwisted ($\phi=0^0$) anti-symmetric angle-ply flat panel subjected to in-plane periodic loads is plotted with non-dimensional frequency Ω/ω (ratio of excitation frequency to the free vibration frequency) without static component of load and compared with the results of Moorthy *et al.* [12]. As observed from Fig 2, the present finite element results show excellent agreement with the previous instability studies.

Table 2 Comparison of non-dimensional fundamental frequencies of vibration of graphite epoxy twisted cantilever plates $[\theta, -\theta, \theta]$ plates, angle of twist $\phi=15^\circ$

$$a/b = 1, E_{11} = 138\text{GPa}, E_{22} = 8.96\text{Gpa}, G_{12} = 7.1\text{GPa}, \nu_{12} = 0.3$$

$$\text{Non dimensional frequency, } \varpi = \omega a^2 \sqrt{(\rho / E_{11} h^2)}$$

b/h	Reference	Non-dimensional fundamental frequencies of free vibration for different ply orientations (θ)						
		$\theta=0^\circ$	$\theta=15^\circ$	$\theta=30^\circ$	$\theta=45^\circ$	$\theta=60^\circ$	$\theta=75^\circ$	$\theta=90^\circ$
100	A	1.0035	0.9296	0.7465	0.5286	0.3545	0.2723	0.2555
	B	1.0034	0.92938	0.74573	0.52724	0.35344	0.27208	0.25544
	C	1.00295	0.92798	0.74381	0.52560	0.35278	0.27200	0.25543
20	A	1.0031	0.8981	0.6899	0.4790	0.3343	0.2695	0.2554
	B	1.0031	0.89791	0.68926	0.47810	0.33374	0.26934	0.25540
	C	0.99107	0.87025	0.67939	0.47143	0.33074	0.26786	0.25506

A=Qatu & Leissa [3], B=He, Lim and Kitipornchai [4] and C= Present work

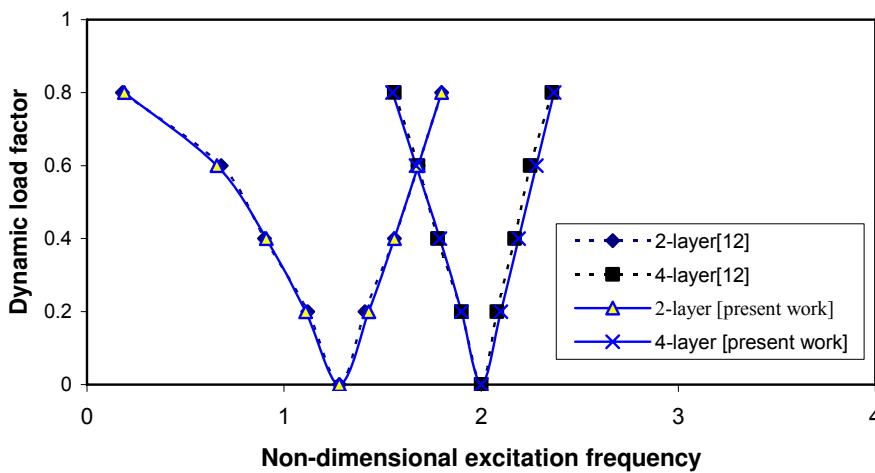


Figure 2 Comparison of instability regions with number of layers of untwisted ($\phi=0^\circ$),

angle-ply panel (two layer: $45^\circ/45^\circ$, four layer: $45^\circ/45^\circ/45^\circ/45^\circ$), $a/b=1$, $\alpha=0.0$.

Numerical results: After validating the formulation, the parametric instability studies are carried out for uniaxially loaded laminated composite pre-twisted panels with static component of load to consider the effect of various parameters. The geometrical and material properties of the cantilever panel are: $a=b=500$ mm, $h=2$ mm (unless otherwise stated).

$$E_{11} = 141.0Gpa, E_{22} = 9.23Gpa, G_{12} = G_{13} = 5.95Gpa, G_{23} = 2.96Gpa, \nu_{12} = 0.313$$

The non-dimensional excitation frequency $\Omega = \bar{\Omega} a^2 \sqrt{(\rho/E_{22}h^2)}$ is used throughout the dynamic instability studies, where $\bar{\Omega}$ is the excitation frequency in radian/second.

The variations of instability regions with static load factor (α) for a twisted anti-symmetric angle-ply panel of square plan-form and twisting angle $\phi=15^\circ$ is shown in Figure 3. As observed in Figure 3, the instability occurs earlier and the width of instability zones expands with increase in static load factor from 0.0 to 0.6. All further studies are done with static load factor $\alpha=0.2$.

The variations of instability regions with ply orientation of angle-ply $[\theta/-\theta/\theta/-\theta]$ cantilevered pre-twisted ($\phi=30^\circ$) panels for uniform loading with static component is shown in Figure 4.

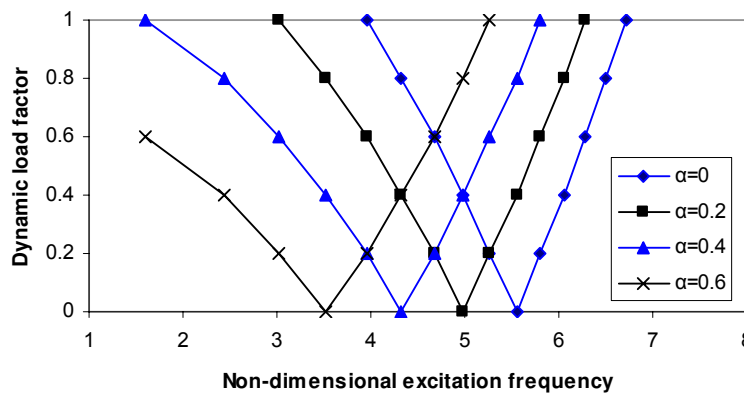


Figure 3 Variations of instability regions with static load factor of a twisted angle-ply panel $[30^\circ/-30^\circ/30^\circ/-30^\circ]$, $a/b=1$, $\phi=15^\circ$, $\alpha=0.0, 0.2, 0.4$ and $\alpha=0.6$.

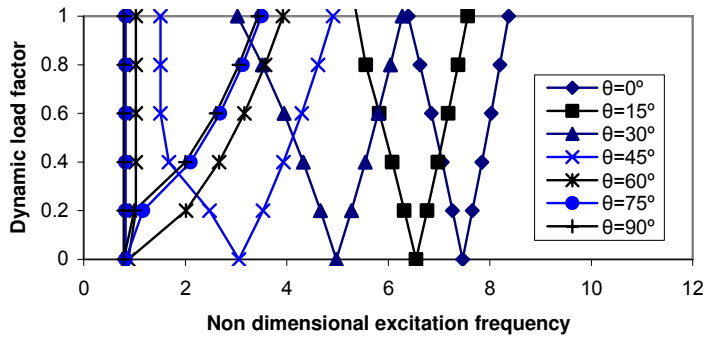


Figure 4 Variations of instability regions with ply orientation of a twisted angle-ply panel $[\theta^\circ/\theta^\circ/\theta^\circ/\theta^\circ]$, $a/b=1$, $\phi=15^\circ$, $\alpha=0.2$, $\theta^\circ=0^\circ$ to 90° .

As observed, the onset of instability occurs earlier for ply orientations of 60° , 75° and 90° . The instability occurs much later for ply orientation of 0° and 15° . The ply orientation 0° seems to be the preferential ply orientation for this lamination sequence and twisting angle. Thus the ply orientations significantly affected the onset of instability region and the width of instability zones. The variation of instability regions shows asymmetric behaviour unlike the results of dynamic stability of simply supported, square and untwisted angle-ply plates by Chen and Yang [11]. This may be due to the un-symmetry in boundary conditions and twisting of the panels.

The dynamic stability regions are plotted for angle-ply $[30^\circ/-30^\circ/30^\circ/-30^\circ]$ twisted panel with different angle of twist i.e. $\phi=0^\circ$, $\phi=15^\circ$ and $\phi=30^\circ$. As shown in Figure 5, the onset of instability occurs earlier with introduction of twist ($\phi=15^\circ$) in the untwisted panel ($\phi=0^\circ$). With increase of twist angle from $\phi=15^\circ$ to $\phi=30^\circ$, the onset of instability occurs earlier with wider instability regions, for this lamination sequence and ply orientation. The dynamic instability regions have been plotted for cantilever angle-ply panel of aspect ratios $a/b=1$, 2 and 4. As shown in Fig.6, the excitation frequency decreases from square ($a/b=1$) to rectangular panels ($a/b=2$ and 4) with increase of aspect ratio.

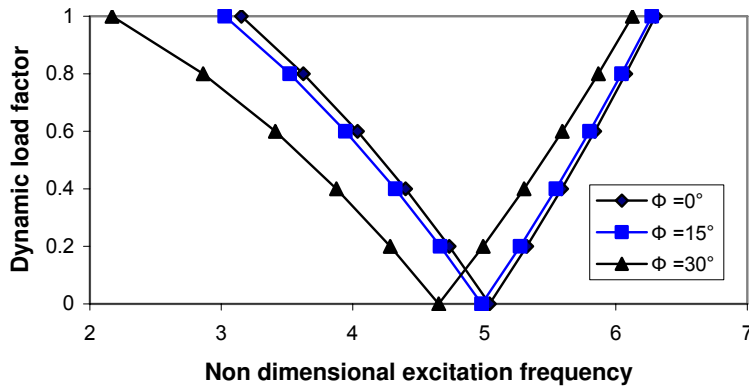


Figure 5 Variations of instability regions with angle of twist of the twisted angle-ply flat panel $[30^\circ/30^\circ/30^\circ/30^\circ]$, $a/b=1$, $\phi=0^\circ, 15^\circ$ and 30° , $\alpha=0.2$.

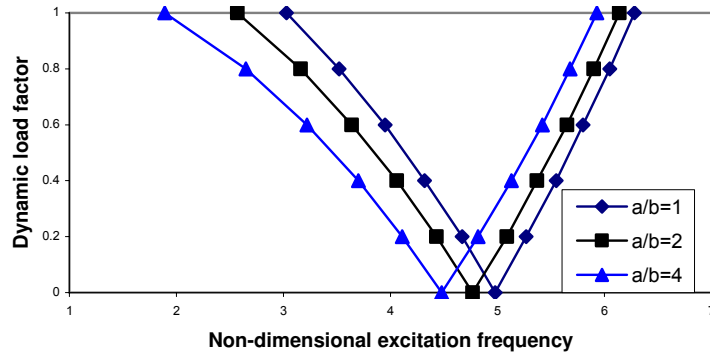


Figure 6 Variations of instability regions with aspect ratio of the twisted angle-ply panel $[30^\circ/30^\circ/30^\circ/30^\circ]$, $a/b=1, 2$ and 4 , $\phi=15^\circ$, $\alpha=0.2$.

The instability regions is also studied for pre-twisted 2, 4 and 8 layer anti-symmetric angle-ply panels. The onset of instability regions occurs later with more number of layers due to the bending stretching coupling. The effect of b/h ratio on the instability regions has been studied for uniform loading with static component. As observed in Fig.7, the onset of instability occurs with a higher excitation frequency for with increase of thickness of panels from $b/h=300$ to $b/h=200$. The width of instability regions is also wider for thinner panels than thicker panels.

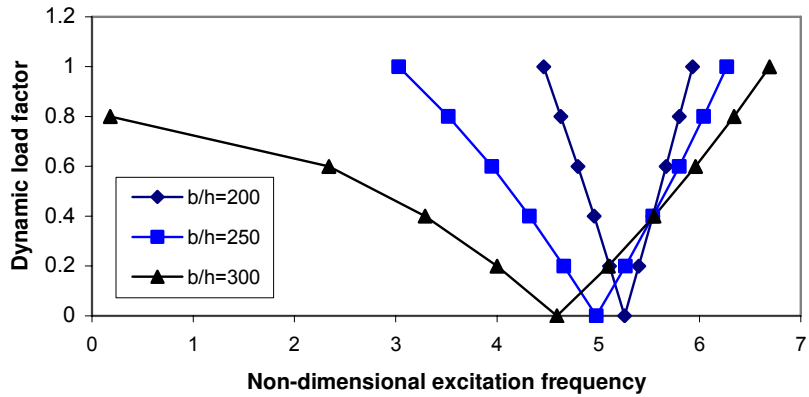


Figure 7 Variations of instability regions with b/h ratio of the twisted angle-ply panel $[30^\circ/30^\circ/30^\circ/30^\circ]$, $a/b=1$, $b/h=200, 250, 300$, $\phi=15^\circ$, $\alpha=0.2$.

The effect of degree of orthotropy is examined for the anti-symmetric angle-ply twisted panel for three cases ($E_1/E_2=15, 25$ and 40). As shown in Figure 8, the onset of instability occurs later with increase of degree of orthotropy. The width of instability zones decrease with increase of degree of orthotropy. The variation of instability regions is studied for anti-symmetric angle-ply pre-twisted cylindrical panels ($b/R_y=0.25$) to study the effect of angle of twist on the curved panel. As seen from Figure 9, there is significant deviation of the instability behaviour of twisted cylindrical panels than that of untwisted panels.

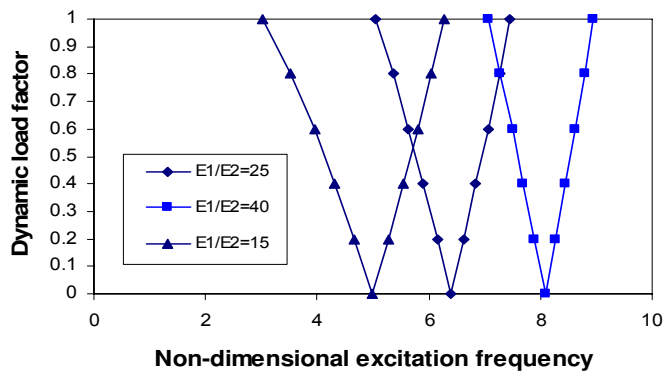


Figure 8 Variations of instability regions with degree of orthotropy (E_1/E_2) of the twisted angle-ply panel $[30^\circ/30^\circ/30^\circ/30^\circ]$, $a/b=1$, $E_1/E_2=15, 25, 40$, $\phi=15^\circ$, $\alpha=0.2$.

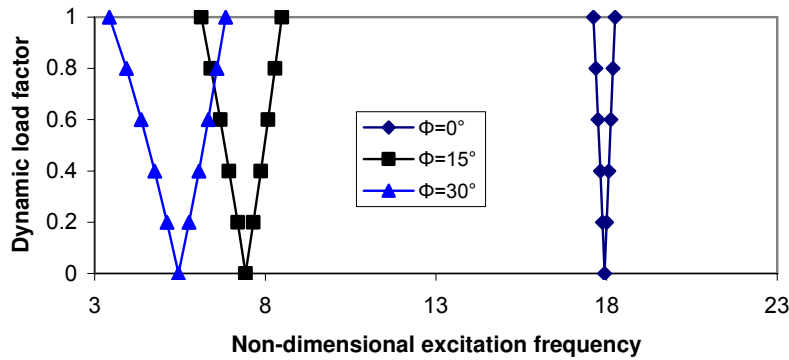


Figure 9 Variations of instability regions of the twisted angle-ply cylindrical panel $[30^\circ/-30^\circ/30^\circ/-30^\circ]$ with angle of twist ($\phi=0^\circ, 15^\circ$ and 30°), $a/b=1$, $\alpha=0.2$.

The onset of instability of twisted cylindrical panels occurs much earlier than untwisted panels. The widths of instability regions increase with increase of angle of twist in the panel. Similar behaviour is also observed for the variation of instability region of twisted spherical and hyperbolic paraboloidal panels. The studies were then extended to compare the dynamic instability regions of different composite cantilever curved panels i.e cylindrical ($b/R_y=0.25$), spherical ($b/R_x=0.25$, $b/R_y=0.25$) and hyperbolic paraboloidal ($b/R_x=-0.25$, $b/R_y=0.25$) panels, for a particular twist ($\phi=15^\circ$), to study the effect of curvature.

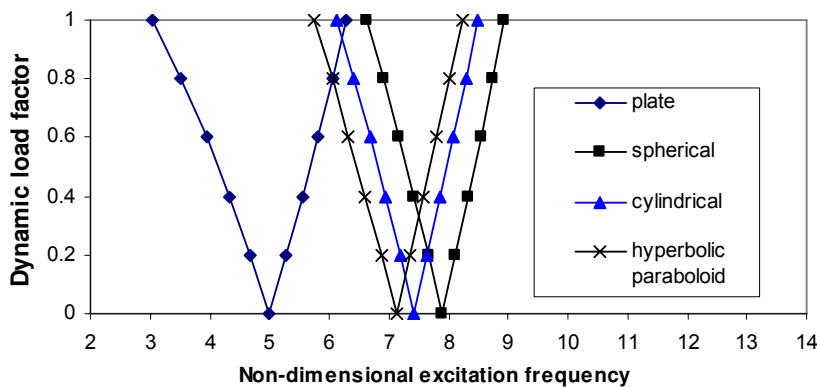


Figure 10 Variations of instability regions with curvature for different twisted curved panels of angle-ply $[30^\circ/-30^\circ/30^\circ/-30^\circ]$ panels, $a/b=1$, $\phi=15^\circ$, $\alpha=0.2$, $b/R_y=0.25$.

As observed from Figure 10, the onset of instability regions occurs later for cylindrical panels than the flat panels due to addition of curvature. The width of instability regions is smaller for cylindrical panels than flat panels. However, the spherical pre-twisted panels show small increase of non-dimensional excitation frequency. The onset of instability of laminated composite pre twisted hyperbolic paraboloidal curved panels occurs earlier to pre twisted cylindrical panels but after flat panels.

4. CONCLUSION

The results on the stability studies of the laminated composite pre-twisted cantilever panels can be summarised as follows:

- Due to static component of load, the onset of instability shift to lower frequencies with wide instability regions of the laminated composite pre-twisted cantilever panels.
- The angles of lamination significantly affect the instability behaviour of uniaxially loaded angle-ply twisted cantilever panels. It shows asymmetrical behaviour due to non-symmetric boundary condition and twisting of panels.
- The onset of instability occurs earlier with introduction of twist ($\phi=15^\circ$) in the otherwise untwisted flat panel ($\phi=0^\circ$). There is significant variation of dynamic instability regions if the angle of twist of the panel changes from $\phi=15^\circ$ to a panel with $\phi=30^\circ$ for this lamination sequence and ply orientation.
- The onset of instability occurs earlier with introduction of twist in the composite panels. The effect of twist is more pronounced in curved panels than flat panels.
- The onset of instability occurs later for pre-twisted square panels than rectangular panels with increase of aspect ratio. The width of dynamic instability region is smaller for square panels than rectangular ones.

- The laminated composite pre-twisted cantilever panels become more stiff with more number of layers.
- The onset of instability occurs with a smaller non-dimensional frequency for thin twisted panels than thick panels. The widths of instability regions are much less for thick panels than corresponding thin panels.
- The instability occurs later along with reduction in width of dynamic instability regions with increase of orthotropy.
- The onset of instability regions occurs later for cylindrical panels than the flat panels due to addition of curvature. However, the spherical pre-twisted panels show small increase of non-dimensional excitation frequency. The onset of instability of hyperbolic parabolic curved panels occurs earlier to pre twisted cylindrical panels but after flat panels.

From the above studies, it may be concluded that the instability behaviour of composite twisted cantilever panels is greatly influenced by the geometry, material, angle of twist and lamination parameters. So, this can be used to the advantage of tailoring during design of composite twisted cantilever panels.

5. REFERENCES

1. A.W. Leissa, Vibrational aspects of rotating turbo-machinery blades, *Appl. Mech. Rev.*, **34** (1981) 629-635.
2. A.W. Leissa, J.K. Lee and A.J Wang, Rotating blade vibration analysis using shells *ASME J. Eng Power*, **104** (1982), 296-302.
3. M.S. Qatu and A.W. Leissa, Vibration studies for laminated composite twisted cantilever plates, *Int J. Mech Science*, **33** (1991), 927-940.
4. L.H. He, C.W. Lim and S. Kitipornchai, A non discretized global model for free vibration of generally Laminated fibre reinforced pre twisted cantilever plates, *Computational Mechanics*, **26** (2000), 197-207.

5. A. Karmakar and P.K. Sinha, Finite Element free vibration analysis of rotating Laminated composite pre-twisted cantilever plates, *Journal of Reinforced plastics and composites*, **16** (1997), 1461-1490.
6. X.X. Hu, T. Sakiyama, C.W. Lim, Y. Xiong, H. Matsuda, C. Morita, Vibration of angle-ply laminated plates with twist by Raleigh-Ritz procedure, *Computer Methods in Applied Mechanics and Engineering*, **193**, (2004), 805-823.
7. Y. J. Kee, J.H. Kim. Vibration characteristics of initially twisted rotating shell type composite blades, *Composite structures*, **64**, (2004), 151-159.
8. J.J. Lee, C.H. Yeom, L. Lee, Vibration analysis of twisted cantilevered conical composite shells, *Journal of Sound and Vibration*, **255** (2002), 965-982.
9. X. Hu, T. Sakiyama, H. Matsuda, C. Morita, Vibration of twisted laminated composite conical shells, *International Journal of Mechanical Sciences*, 2002; **44**: 1521-1541.
10. V. V. Bolotin, *The Dynamic Stability of Elastic System*, San Francisco: Holden-Day. 1964.
11. L.W. Chen and J.Y. Yang, Dynamic stability of laminated composite plates by the finite element method, *Computers and Structures*, **36**(5) (1990), 845-851.
12. J. Moorthy, J.N. Reddy and R.H. Plaut, Parametric instability of laminated composite plates with transverse shear deformation, *International Journal of Solids and Structures*, **26** (1990), 801-811.
13. G. Cederbaum, Dynamic stability of shear deformable laminated plates, *AIAA Journal*, **29** (1991), 2000-2005.
14. S. K. Sahu and P.K. Datta, Dynamic instability of laminated composite rectangular plates subjected to non-uniform harmonic in-plane edge loading, *Journal of*

- Aerospace Engg., Proc. Of Institution of Mechanical Engineers, Part G*, **214** (2000), 295-312.
15. M. Ganapathi, T.K. Varadan and V. Balamurugan, Dynamic stability of laminated composite curved panels using finite element method, *Computers and Structures*, **53** (2)(1994), 335-342.
 16. S.K. Sahu and P.K. Datta. Parametric resonance characteristics of laminated composite doubly curved shells subjected to non-uniform loading, *Journal of Reinforced Plastics and Composites*, **20**(18)(2001), 1556-1576.
 17. R.C. Kar and K. Ray, Dynamic stability of a pre-twisted, three layered symmetric sandwich beam, *Journal of Sound and Vibration*, **183**(4)(1995), 591-606.
 18. L.W. Chen and W.K. Peng, Dynamic stability of rotating blades with geometric non-linearity, *Journal of Sound and Vibration*, **187**, (1995), 421-433.
 19. Lin Chung-Yi and Chen Lien-wen, Dynamic stability of rotating pre-twisted blades with a constrained damping layer, *Composite Structures*, **61**, (2003), 235-245.
 20. D.J. Crispino and R.C. Benson, Stability of twisted orthotropic plates, *International Journal of Mechanical Sciences*, 28 (6), 371-379.
 21. S. K. Sahu, A.V. Asha and R.N. Mishra, Stability of laminated composite pretwisted cantilever panels, *Journal of Reinforced Plastics and Composites*, **24**, (2005),1327-1334.
 22. S. K. Sahu, P.K. Datta, Dynamic stability of laminated composite curved panels with cutouts, *Journal of Engineering Mechanics, ASCE*, **129**(11)(2003), 1245-1253.
 23. Reddy JN. *Mechanics of Laminated Composite plates and Shells*, CRC Press, Washington, 2004.

Legends of Figures

Figure 1 Geometry and co-ordinate systems of twisted cantilever plates.

Figure 2 Comparison of instability regions with number of layers of untwisted ($\phi=0^\circ$),

angle-ply panel (two layer: $45^\circ/45^\circ$, four layer: $45^\circ/45^\circ/45^\circ/45^\circ$), $a/b=1$, $\alpha=0.0$.

Figure 3 Variations of instability regions with static load factor of a twisted angle-ply panel

$[30^\circ/30^\circ/30^\circ/30^\circ]$, $a/b=1$, $\phi=15^\circ$, $\alpha=0.0, 0.2, 0.4$ and $\alpha=0.6$.

Figure 4 Variations of instability regions with ply orientation of a twisted angle-ply

panel $[\theta^\circ/\theta^\circ/\theta^\circ/\theta^\circ]$, $a/b=1$, $\phi=15^\circ$, $\alpha=0.2$, $\theta^\circ=0^\circ$ to 90° .

Figure 5 Variations of instability regions with angle of twist of the twisted angle-ply flat

panel $[30^\circ/30^\circ/30^\circ/30^\circ]$, $a/b=1$, $\phi=0^\circ, 15^\circ$ and 30° , $\alpha=0.2$.

Figure 6 Variations of instability regions with aspect ratio of the twisted angle-ply panel

$[30^\circ/30^\circ/30^\circ/30^\circ]$, $a/b=1, 2$ and 4 , $\phi=15^\circ$, $\alpha=0.2$.

Figure 7 Variations of instability regions with b/h ratio of the twisted angle-ply panel

$[30^\circ/30^\circ/30^\circ/30^\circ]$, $a/b=1$, $b/h=200, 250, 300$, $\phi=15^\circ$, $\alpha=0.2$.

Figure 8 Variations of instability regions with degree of orthotropy (E_1/E_2) of the twisted angle-

ply panel $[30^\circ/30^\circ/30^\circ/30^\circ]$, $a/b=1$, $E_1/E_2=15, 25, 40$, $\phi=15^\circ$, $\alpha=0.2$.

Figure 9 Variations of instability regions of the twisted angle-ply cylindrical panel

$[30^\circ/30^\circ/30^\circ/30^\circ]$ with angle of twist ($\phi=0^\circ, 15^\circ$ and 30°), $a/b=1$, $\alpha=0.2$.

Figure 10 Variations of instability regions with curvature for different twisted curved panels of

angle-ply $[30^\circ/-30^\circ/30^\circ/-30^\circ]$ panels, $a/b=1$, $\phi=15^\circ$, $\alpha=0.2$, $b/R_y=0.25$.

Legends of Tables

Table 1 Convergence of non-dimensional fundamental frequencies of vibration of

composite twisted cantilever plates with $[45^\circ/-45^\circ/45^\circ]$ lamination.

Table 2 Comparison of non-dimensional fundamental frequencies of vibration of

graphite epoxy twisted cantilever plates $[\theta, -\theta, \theta]$ plates.